JOURNAL OF MAGNETIC RESONANCE, Series A 107, 50–55 (1994)

Homo- and Heteronuclear Multiple-Quantum Filters for Measurement of NMR Isotope Shifts

E. WRENN WOOTEN,*†‡ RAJESH K. DUA,* GARRY D. DOTSON,* AND RONALD W. WOODARD*

*College of Pharmacy and †Biophysics Research Division, The University of Michigan, Ann Arbor, Michigan 48109

Received April 26, 1993; revised June 17, 1993

The measurement of NMR isotope shifts as mechanistic probes can be complicated by mixtures of isotopomers. Homo- and heteronuclear NMR techniques based on multiple-quantum filtration are presented and shown to be a useful aid in measuring such shifts. The effects of $^{1}H/^{2}H$ substitution and $^{16}O/^{18}O$ substitution on the nuclear shielding of ^{1}H, ^{13}C, and ^{31}P in a multiply labeled phosphoenolpyruvate are measured and interpreted qualitatively in terms of their rovibrational origins.

INTRODUCTION

The effect of isotopic substitution on nuclear shielding has long been used as a probe in mechanistic chemistry and enzymology (*1–3*). For example, the difference in the shift of ^{13}C when directly bonded to ^{16}O or ^{18}O is often used to determine whether a C–O bond is broken during a chemical reaction (*1*). Observation and measurement of isotope shifts are typically carried out using a single NMR tube containing the labeled and unlabeled species. As previously pointed out, however, one major obstacle in such studies is the presence of mixtures of isotopically labeled species (*3*). Mixtures often arise from incomplete stereo- or regiospecificity of the labeling method. The spectral complexity resulting from the combined effects of scalar couplings and multiple isotope shifts can often make the observation of the desired shift extremely difficult. This can be especially problematic when ^{18}O-labeled water is used to incorporate ^{18}O by acid-catalyzed exchange. The use of "unnormalized" water provides a much cheaper and more readily available source of ^{18}O than its "normalized" counterpart; however, the unnormalized reagent typically contains >90% deuterium, which usually becomes incorporated to some degree during the exchange. Several NMR spectral-editing techniques have been suggested to circumvent the problem of mixtures and have largely involved using spin echos (*4, 5*), DEPT-based methods (*6, 7*), or extensions of the two (*7*). Here we present editing techniques based on multiple-quantum filtration (MQF).

‡ To whom correspondence should be addressed.

Homonuclear multiple-quantum filtration (HoMQF) techniques (*8, 9*) are well-established for spectral simplification and are often used as a means to simplify the spectra of biopolymers. HoMQF typically involves the creation of multiple-quantum coherences between protons. The coherences are then separated and detected (usually indirectly) on the basis of their responses to the phase of RF pulses on the protons. Heteronuclear multiple-quantum filtration (HeMQF) is a similar technique closely related to INEPT (*10*), DEPT (*11, 12*), and methods like them (*13*), except MQF uses phase shifts instead of flip angles for spin system discrimination. HeMQF involves creating multiple-quantum coherences between, for example, protons and one or more X nuclei. In contrast to HoMQF, the coherences are then separated and detected (usually indirectly) according to the RF phase of the proton pulses, the X pulses, or both. Multiple-quantum filtration methods are therefore useful as "molecular selectors" to select out subspectra corresponding to individual populations of molecules, because the possible multiple-quantum coherences that can be created are determined by the coupling topology of the molecule and the values of the scalar coupling constants. We show that by using homo- and heteronuclear multiple-quantum filtration, we can obtain subspectra for the various isotopomers in a multiply isotopically labeled phosphoenolpyruvate. In so doing, we can measure precisely the effects of $^{1}H/^{2}H$ substitution and $^{16}O/^{18}O$ substitution on the nuclear shielding of ^{1}H, ^{13}C, and ^{31}P.

MATERIALS AND METHODS

Synthesis of [2-^{13}C,2-^{18}O,3,3-H(D)]Phosphoenolpyruvate

[2-^{13}C]Sodium pyruvate (99%), purchased from Cambridge Isotope Laboratory, was suspended in CCl_4, first converted into pyruvic acid by the addition of 1.1 equivalent of concentrated HCl and then into bromopyruvic acid by treatment with bromine via the method reported by Stubbe and Kenyon (*14*). The 3-bromo-[2-^{13}C]pyruvic acid was converted into 3-[2-^{13}C, 2-^{18}O, 3,3-H(or D)]bromopyruvate by the exchange method of Sprinson *et al.* (*15*) except that

1064-1858/94 $6.00

unnormalized water, purchased from Cambridge Isotope Laboratory (^{18}O, 98%; D, 90%), was utilized. The NaCl present from the initial sodium salt was removed by filtration once the labeled bromopyruvic acid was dissolved in anhydrous diethyl ether. The ethereal solution of labeled bromopyruvic acid was converted into enolpyruvyl phosphate by treatment with $P(OCH_3)_3$ under Perkov reaction conditions and then into its monocyclohexylamine salt by the method reported by Clark and Kirby (*16*). The melting point range was 143–144°C, in agreement with the previously published range of 143–146°C (*17*). The compound was seen to be pure by NMR. The structure of phosphoenolpyruvate (PEP) and the isotopic labeling positions are shown in Fig. 1. The resulting compound is a mixture of labeled molecules with varying degrees of incorporation of deuterium and ^{18}O, giving rise to as many as eight possible structures.

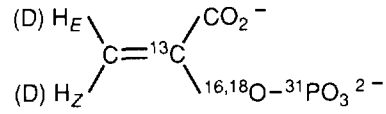

FIG. 1. Molecular structure of phosphoenolpyruvate (PEP) showing sites of isotopic substitution. There are two monodeuterated (E and Z monoprotio) species and one undeuterated (diprotio) species present. No dideuterated species was detected.

NMR Spectroscopy

Nuclear magnetic resonance spectra were recorded on the monocyclohexylamine salt on a Bruker AMX500 spectrometer (11.75 T) at a probe temperature of 298 K using 5 mm high-resolution NMR tubes. Sample volumes were 500 μl at a concentration of 10 mg/ml in deuterium oxide (100 at%). For ^1H spectra, a spectral width of 3000 Hz was employed, while for ^{13}C and ^{31}P, a spectral width of 2000 Hz was used. Spectra were obtained with a 1.0 s relaxation delay and 16,384 complex points in the time domain using simultaneous detection of real and imaginary components. The GARP sequence (*18*) was used for heteronuclear decoupling. The time-domain data were apodized with an exponential (0.5 Hz for X nuclei) prior to zero-filling followed by Fourier transformation. The pulse sequences and phase cycles used are shown in Fig. 2.

Figure 2a shows the pulse sequence, phase cycle, and coherence-transfer pathways (*19*) used to obtain ^1H subspectra for the diprotio and monoprotio (E and Z) PEP species via HoMQF. The first pulse creates transverse magnetization which evolves under the proton chemical shifts and the homo- and heteronuclear scalar couplings. The second pulse refocuses all except the homonuclear coupling. The antiphase term due to this coupling reaches a maximum at the end of the second τ period for $\tau = 1/4J_{HH}$, when the third pulse converts the antiphase coherence into a linear combination of homonuclear zero-, single-, and double-quantum coherences. The fourth pulse then converts nonobservable coherence into single-quantum coherence and, together with the appropriate addition of signals in the receiver (*19*), serves to select or reject one or more of the coherence orders. The final τ—π—τ sequence allows the antiphase single-quantum coherence created by the fourth pulse to evolve into in-phase coherence prior to detection.

Figure 2b shows the pulse sequence, phase cycle, and coherence-transfer pathways used to obtain ^{13}C and ^{31}P subspectra for the diprotio and monoprotio species of PEP via HeMQF. The first pulse creates transverse X magnetization which evolves under the X chemical shift and the heteronuclear scalar coupling. After a period $\tau = 1/4J_{XH}$, the simultaneous carbon and proton π pulses (pulses 2 and 3) refocus all interactions except that due to the XH scalar coupling, and at the end of the second τ period, the antiphase XH coherence has reached its maximum amplitude. The first proton $\pi/2$ pulse (pulse 4) converts the proton longitudinal magnetization into transverse proton magnetization, thereby creating heteronuclear zero-, single-, double-, and triple-quantum coherence. The second proton $\pi/2$ pulse creates observable magnetization and selects or rejects the desired multiple-quantum coherence with proper addition in the receiver as before. The final τ—π—τ sequence converts the single-quantum antiphase coherence into in-phase coherence, which is then detected. It is important to note that since the J_{XH} values are approximately equal for the Eand Z protons, τ is set to the same value in both the heteronuclear double- and triple-quantum filters for maximum generation of the highest coherence order possible in each molecular species, owing to the $\sin(\pi J2\tau)$ and $\sin^2(\pi J2\tau)$ dependences of the double- and triple-quantum coherences in the mono- and diprotio species, respectively. The double-quantum coherence of the diprotio species has a $\sin(\pi J2\tau)\cos(\pi J2\tau)$ dependence which has zero amplitude for $\tau = 1/4J_{XH}$.

RESULTS

Figure 3a shows the unfiltered ^1H spectrum of PEP (i), the ^1H spectrum of the diprotio species obtained by homonuclear double-quantum filtration (ii), and the monoprotio species obtained by homonuclear single-quantum filtration (iii). Figure 3b shows the unfiltered ^1H-decoupled ^{13}C spectrum of PEP (i), the ^{13}C spectrum of the diprotio species obtained by heteronuclear triple-quantum filtration (ii), and the monoprotio species obtained by heteronuclear double-quantum filtration (iii). Figure 3c gives the analogous spectra for ^{31}P. No evidence for significant amounts of the dideutero compound was seen either in the unfiltered spectrum or by heteronuclear single-quantum filtration. Addition of the subspectra gives a sum comparable to the unfiltered spectrum in all three cases. The sets of proton subspectra allow the effects of deuterium on the proton chemical shifts to be ob-

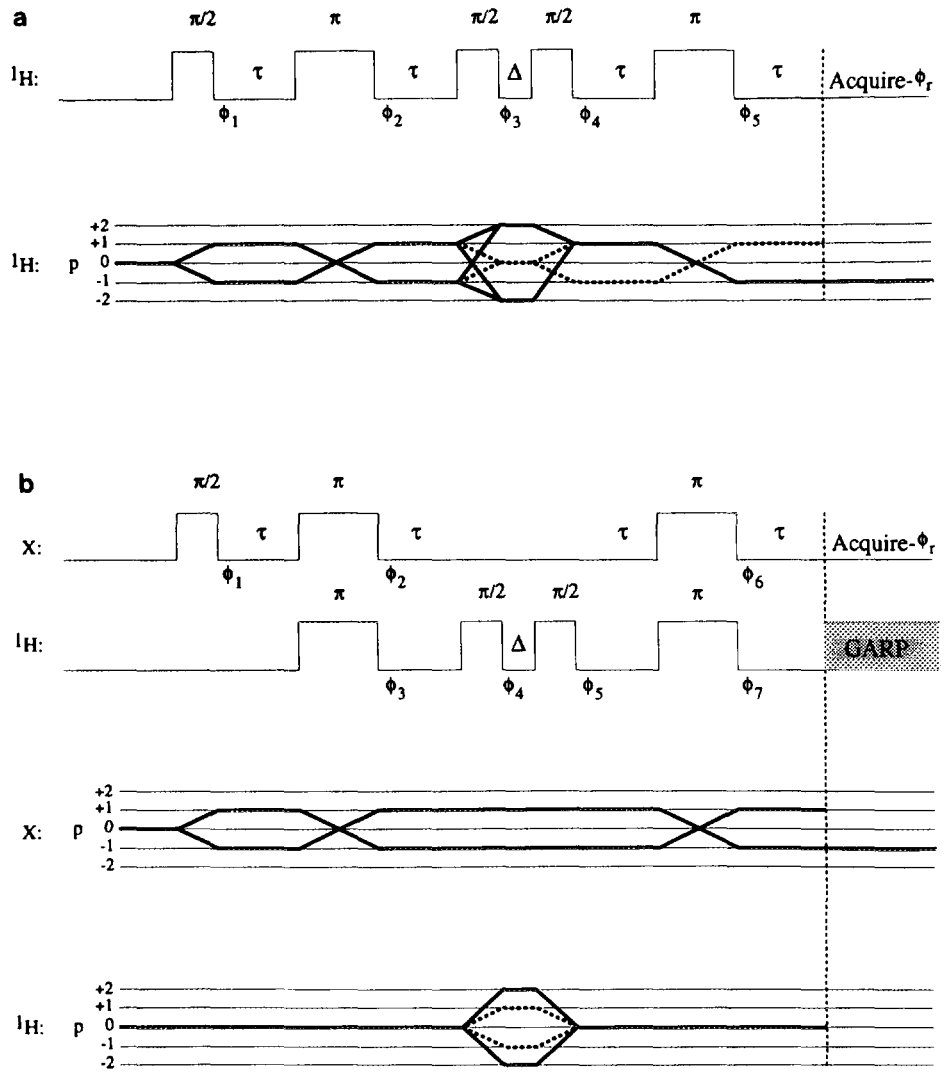

FIG. 2. Pulse sequences and coherence-transfer pathways for homo- and heteronuclear multiple-quantum filters. In (a) the bold lines show the pathways for extracting the ^{1}H subspectrum of the diprotio species (^{1}H–^{1}H double-quantum filter) with phase cycle $\phi_1 = \phi_2 = \phi_3 = \phi_5 = 0$; $\phi_4 = 0, \pi/2, \pi, 3\pi/2$; $\phi_r = 0, \pi/2, \pi, 3\pi/2$. The dotted lines show the pathways for extracting the subspectrum of the monoprotio species (^{1}H single-quantum filter) with phase cycle $\phi_1 = \phi_2 = \phi_3 = \phi_5 = 0$; $\phi_4 = 0, \pi/2, \pi, 3\pi/2$; $\phi_r = 0, 3\pi/2, \pi, \pi/2$. In (b) the bold lines show the pathways for extracting the X-nucleus subspectrum of the diprotio species (X–^{1}H–^{1}H triple-quantum filter) with phase cycle $\phi_1 = \phi_2 = \phi_3 = \phi_4 = \phi_6 = \phi_7 = 0$; $\phi_5 = 0, \pi$; $\phi_r = 0$. The dotted lines show the pathways for extracting the subspectrum of the monoprotio species (X–^{1}H double-quantum filter) with phase cycle $\phi_1 = \phi_2 = \phi_3 = \phi_4 = \phi_6 = \phi_7 = 0$; $\phi_5 = 0, \pi$; $\phi_r = \pi, 0$.

tained. More interestingly, the X-nucleus subspectra allow the isotope shift from substitution with an isotope at one site to be measured in the presence and absence of substitution at another site with a different isotope. The various isotope shifts are tabulated in Table 1. The convention for the sign of the isotope shift is that used by Hansen (*3*), $\Delta X(Y) = \delta X(L) - \delta X(H)$. ΔX is the isotope shift on X when substituted by an isotope Y, while $\delta X(L)$ and $\delta X(H)$ are the X chemical shifts when substituted by the light and heavy isotopes, respectively. Scalar coupling constants are given in Table 2 and do not, within experimental error, reveal any isotope effects.

DISCUSSION

The unfiltered spectra in Fig. 3(i) demonstrate the difficulty of precise measurement of isotope effects in multiply isotopically labeled mixtures. This is especially pronounced in the case of phosphorus [Fig. 3c(i)]. Nonetheless, the spectra in Fig. 3(ii and iii) show that MQF can give good subspectra for the various components.

From the spectra in Fig. 3a, the deuterium isotope effect on the proton shielding is easily observed. In the diprotio species [Fig. 3a(ii)], the lines are complicated multiplets due to the scalar coupling of each proton to the other proton,

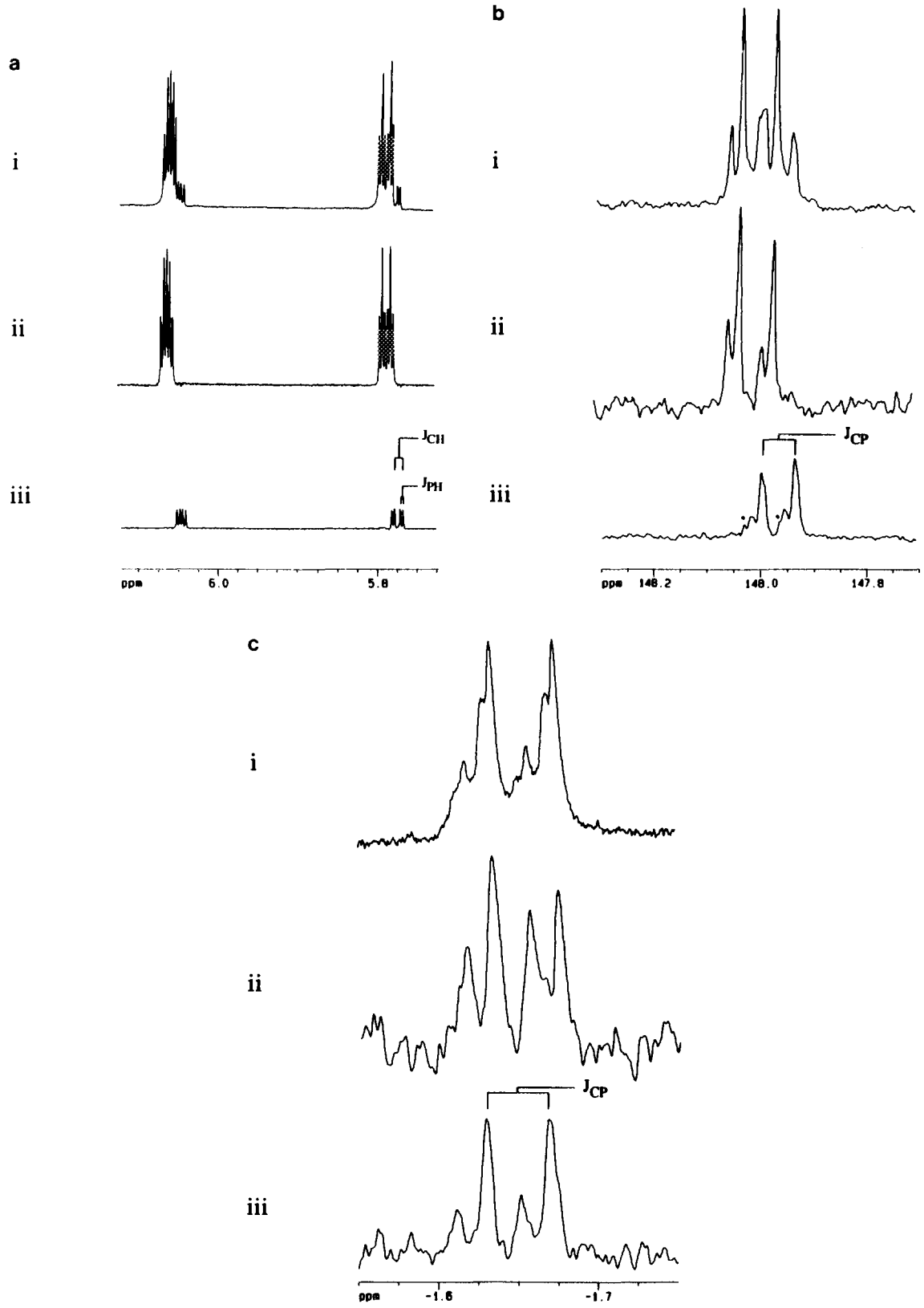

FIG. 3. Unfiltered (i), diprotio (ii), and monoprotio (iii) species subspectra observing ^{1}H (a), ^{13}C (b), and ^{31}P (c).

TABLE 1

Isotope Shifts for Observed Nuclei in PEP for Various Combinations of Isotopic Substitutions A, B, C, D, and E

Observed nucleus	Isotope shifts (ppm ± 0.001)				
	A ($^{16}O/^{18}O$,H)	B ($^{16}O/^{18}O$,D)	C (H/D,^{16}O)	D (H/D,^{18}O)	E ($^{16}O/^{18}O$/D)
^{1}H (E proton)	<0.001	<0.001	0.013	0.013	0.013
^{1}H (Z proton)	<0.001	<0.001	0.013	0.013	0.013
^{13}C	0.019	0.020	0.031	0.032	0.051
^{31}P	0.018	0.019	−0.006	−0.005	0.013

Note. As described under Results, the convention for the sign of the isotope shift is $\Delta X(Y) = \delta X(L) - \delta X(H)$. The nomenclature found in parentheses is defined as follows: ($^{16}O/^{18}O$,H) and ($^{16}O/^{18}O$,D) represent the isotope shifts upon substitution of ^{16}O with ^{18}O in the diprotio and monoprotio forms, respectively. (H/D,^{16}O) and (H/D,^{18}O) represent substitution of H with D in the ^{16}O and ^{18}O forms, respectively. ($^{16}O/^{18}O$/D) represents substitution of H and ^{16}O with D and ^{18}O.

to the carbon, and to the phosphorus. In the monoprotio case [Fig. 3a(iii)], there is no homonuclear proton coupling, and the lines appear as a doublet of doublets due to the two-bond proton–carbon coupling and the four-bond proton–phosphorus coupling. The heteronuclear coupling constants are easily measured, and stereospecific proton–carbon and proton–phosphorus couplings are present (Table 2). The intensities of the E and Z protons in the monoprotio species are roughly equal, indicating as expected a lack of stereospecificity of incorporation. The $^{16}O/^{18}O$ isotope effect on the protons is too small to observe.

In Figs. 3b and 3c, the X nuclei each gives rise to two sets of doublets. The doublet of lower intensity at lower field arises from the X nucleus split by the heteronuclear $J_{XX'}$ coupling in molecules with ^{16}O, while the more intense upfield doublet arises from molecules labeled with ^{18}O. In the ^{13}C subspectrum of the diprotio species [Fig. 3b(iii)], the small peak at the most downfield part of each part of the doublet (marked with a ●) probably derives from some of the more abundant diprotio species getting through the double-quantum filter. It is also possible to see shoulders on the lines in this spectrum, which probably arise from a stereospecific isotope effect depending on whether the deuterium is in the E or Z position. The same effect is more difficult to observe in the phosphorus spectrum [Fig. 3c(iii)] due to the broader lines.

TABLE 2

Homo- and Heteronuclear Scalar Coupling Constants in PEP for Various Combinations of Isotopic Substitutions A, B, C, and D

Coupling pair	Coupling constants (Hz ± 0.05)			
	A (^{16}O,H)	B (^{16}O,D)	C (^{18}O,H)	D (^{18}O,D)
^{13}C–^{31}P	8.09	8.05	8.15	8.06
^{13}C–^{1}H (E proton)	nd	3.91	nd	3.91
^{13}C–^{1}H (Z proton)	nd	5.37	nd	5.37
^{31}P–^{1}H (E proton)	nd	2.08	nd	2.08
^{31}P–^{1}H (Z proton)	nd	1.71	nd	1.71

Note. The nomenclature found in parentheses is defined as follows: (^{16}O,H) and (^{16}O,D) represent the coupling constants in the diprotio and monoprotio forms with ^{16}O, while (^{18}O,H) and (^{18}O,D) represent the corresponding coupling constants for forms with ^{18}O. nd, not determined.

Isotope effects on nuclear shielding are rovibrational in origin and are dependent upon two parameters (*20–22*); the first is the change in shielding with bond extension (the electronic part), and the second is the mass-related effect of the average equilibrium bond length on the shielding (the dynamic part). The isotope shifts obtained here are consistent with those obtained by previous studies for ^{1}H, ^{13}C, and ^{31}P (*3, 23*). The one-bond isotope effects are positive, in accord with the observation that primary electronic contributions, the derivative of the shielding at the observation site with respect to bond displacement due to substitution at the same site, are typically negative in such cases (*20*). The negative four-bond ^{31}P–D isotope effect is also in agreement with some previously observed long-range effects (*24, 25*), since long-range shifts involve secondary electronic components such as the derivative of the shift at the observed nucleus with respect to remote bond displacement, or a secondary dynamic component from changes in local bond length upon remote substitution (*22*). These secondary effects will not necessarily be the same sign or magnitude for most systems, since they depend more upon molecular electronic structure than do primary effects.

Two additional observations also bear special mention and suggest that the contribution of the secondary dynamic effect is in fact small. The first is that the isotope effect due to substitution with one isotope at one site is not affected by the presence of another isotope at another site. For example, comparison of columns A and B in Table 1 reveals that the isotope effect due to a $^{16}O/^{18}O$ substitution is the same for the diprotio and monoprotio species. This first observation directly implies the second, which is that the total isotope effect due to substitution at different sites with different iso-

topes is additive. This is demonstrated by the observation, for example, that in Table 1, columns A and C or columns B and D add up to give column E within experimental uncertainty. These last two observations can be attributed to small secondary dynamic factors; that is, the average ^{13}C–O and ^{31}P–O bond lengths do not change due to $^{1}H/D$ substitution, and likewise for the ^{1}H–^{12}C bond length upon $^{16}O/^{18}O$ substitution. Such changes have been shown to be typically at least two orders of magnitude smaller than primary dynamic effects, the change in average bond length at the site of substitution (*26*). Finally, we note that while we have applied HeMQF to the measurement of NMR isotope effects, it is equally applicable to other situations where it is desirable to observe molecular subspectra within a complex mixture.

ACKNOWLEDGMENTS

We acknowledge helpful discussions with Professor E. R. P. Zuiderweg and his group. We also thank Professor C. J. Jameson for useful discussions concerning isotope effects. Acknowledgment is made to the Donors of The Petroleum Research Fund, administered by the American Chemical Society, for partial support of this research (E.W.W.). R.W.W. is funded by U.S. Public Health Service Grant GM 42544. G.D.D. was supported by U.S. Public Health Training Grant 5-T32-GM-07767 and a Michigan Merit Fellowship from the Rackham Graduate School. We thank the Department of Chemistry at The University of Michigan for access to their AMX500 spectrometer.

REFERENCES

1. J. M. Risley and R. L. Van Etten, *Methods Enzymol.* **177,** 376 (1989).
2. J. J. Villafranca, *Methods Enzymol.* **177,** 390 (1989).
3. P. E. Hansen, *Prog. NMR Spectrosc.* **20,** 207 (1988).
4. T. T. Nakashima and D. L. Rabenstein, *J. Magn. Reson.* **47,** 339 (1982).
5. D. M. Doddrell, J. Staunton, and E. D. Laue, *J. Magn. Reson.* **52,** 523 (1983).
6. T. T. Nakashima, R. E. D. McClung, and B. K. John, *J. Magn. Reson.* **58,** 27 (1984).
7. D. M. Doddrell, J. Staunton, and E. D. Laue, *J. Chem. Soc. Chem. Commun.,* 602 (1983).
8. U. Piantini, O. W. Sørensen, and R. R. Ernst, *J. Am. Chem. Soc.* **104,** 6800 (1982).
9. O. W. Sørensen, M. H. Levitt, and R. R. Ernst, *J. Magn. Reson.* **55,** 104 (1983).
10. G. A. Morris and R. Freeman, *J. Am. Chem. Soc.* **101,** 760 (1979).
11. D. M. Dodrell, D. T. Pegg, and M. R. Bendall, *J. Magn. Reson.* **48,** 323 (1982).
12. M. R. Bendall and D. T. Pegg, *J. Magn. Reson.* **53,** 272 (1983).
13. R. R. Ernst, G. Bodenhausen, and A. Wokaun, "*Principles of Nuclear Magnetic Resonance in One and Two Dimensions,*" Clarendon Press, Oxford, 1987.
14. J. Stubbe and G. L. Kenyon, *Biochemistry* **10,** 2669 (1971).
15. W. E. Bondinell, J. Vnek, P. F. Knowles, M. Sprecher, and D. B. Sprinson, *J. Biol. Chem.* **246,** 6191 (1971).
16. V. M. Clark and A. J. Kirby, *Biochim. Biophys. Acta* **78,** 732 (1963).
17. A. E. Woods, J. M. O'Bryan, P. T. K. Mui, and R. D. Crowder, *Biochemistry* **9,** 2334 (1970).
18. A. J. Shaka, P. B. Barker, and R. Freeman, *J. Magn. Reson.* **64,** 547 (1985).
19. G. Bodenhausen, H. Kogler, and R. R. Ernst, *J. Magn. Reson.* **58,** 370 (1984).
20. C. J. Jameson, *J. Chem. Phys.* **66,** 4977 (1977).
21. C. J. Jameson, *J. Chem. Phys.* **66,** 4983 (1977).
22. C. J. Jameson and J. Osten, *Annu. Rep. NMR Spectros.* **17,** 1 (1986).
23. P. E. Hansen, *Annu. Rep. NMR Spectros.* **15,** 105 (1983).
24. A. R. Siedle and R. A. Newmark, *J. Am. Chem. Soc.* **111,** 8010 (1989).
25. S. G. Lee and S. E. Yoo, *Bull. Korean Chem. Soc.* **10,** 393 (1989).
26. C. J. Jameson and J. Osten, *J. Chem. Phys.* **81,** 4293 (1984).